Available online at www.sciencedirect.com
SCIENCE DIRECT®
Journal of Crystal Growth 267 (2004) 85–91
JOURNAL OF CRYSTAL GROWTH
www.elsevier.com/locate/jcrysgro

The effect of ZnO homo-buffer layer on ZnO thin films grown on c-Al_2O_3(0 0 0 1) by plasma assisted molecular beam epitaxy

Yeon-Sik Jung, Young-Soo No, Jin-Sang Kim, Won-Kook Choi*

Korea Institute of Science and Technology, Thin Film Materials Research Center, P.O. Box 131, 39-1 Howolgok-dong, Seongbuk-gu, Cheongryang, Seoul 136791, South Korea

Received 3 March 2004; accepted 8 March 2004
Communicated by D.P. Norton

Abstract

ZnO thin films were deposited on *c*-plane sapphire substrates on the ZnO homo-buffer layer with different thickness and growth temperature by plasma assisted molecular beam epitaxy. The effects of buffer-layer growth variables on the properties of the ZnO films were investigated and discussed on a collective basis compared with other reports. RHEED patterns were taken over different buffer layer surfaces and the initial growth mode of ZnO buffer layer was recognized as Stranski–Krastanov mode by the direct observation of a streaky pattern superimposed with a spotty pattern of thicker than 8 nm. Through examining the XRD θ-rocking curve of ZnO (0 0 0 2) peak, it seems that the crystalline quality of the ZnO thin film grown on the ZnO buffer layer was gradually improved with the increase of the buffer layer thickness. Strong near band-edge emission at 378 nm was well observed without deep-level emission at the ZnO films grown on the 15 nm buffer layer prepared at 500–600°C, and those grown on the thicker buffer layer or prepared at 400°C or 700°C showed deep-level emission around 510 nm. In Hall measurement, the ZnO films showing deep-level emission gave also carrier concentration higher than $1 \times 10^{19}/\mathrm{cm}^3$ and those with better crystalline quality seemed to have high mobility of $\mu = 40-57\,\mathrm{cm}^2/\mathrm{V\,s}$.

PACS: 61.10.Nz; 61.14.Hg; 68.55.Jk; 73.61.Ga; 78.66.Hf; 81.15.Hi

Keywords: A1. Crystal structure; A1. Photoluminescence; A1. Reflection high energy electron diffraction; A1. X-ray diffraction; A3. Molecular beam epitaxy; B2. Semiconducting II–VI materials

1. Introduction

ZnO has been noticed as a promising candidate for UV/Blue optical devices [1–3], since it was discovered that the luminescence mechanism of the near band-edge emission (NBE) and the green deep-defect level emission of ZnO are quite analogous to those of GaN [4]. Much interest, in particular, has been paid due to its large exciton binding energy (59 meV) as compared to GaN (28 meV) and its higher optical gain ($300\,\mathrm{cm}^{-1}$) than in GaN ($100\,\mathrm{cm}^{-1}$) at room temperature.

*Corresponding author. Tel.: +82-2-958-5565; fax: +82-2-958-6851.
E-mail address: wkchoi@kist.re.kr (W.-K. Choi).

0022-0248/$ - see front matter © 2004 Elsevier B.V. All rights reserved.
doi:10.1016/j.jcrysgro.2004.03.010

The advantages of low-temperature buffer layer for the growth of high quality epitaxial GaN films on sapphire to reduce the dislocation density has been reported by many researchers [5–7]. The buffer layers grown with appropriate thickness and deposition temperatures showed better electrical, optical, and morphological properties. In pursuit of similar effects and purposes, low-temperature homo-buffer layers for epitaxial ZnO films deposited on sapphire substrates have been tried [8–10]. Nakamura et al. have showed the crucial effect of low-temperature buffer layer on the morphology and crystallinity of ZnO films deposited by pulsed laser deposition [9]. Nakahara et al. also reported that high temperature growth of ZnO films on sapphire was possible only when initial low-temperature buffer layer was introduced during the deposition by radical-source MBE [8].

However, the effects on morphological, optical, structural, and electrical properties of ZnO films by differing the buffer-layer deposition variables of molecular beam epitaxy (MBE), which is a common deposition tool for high quality epitaxial films, have not been systematically examined yet.

Thus, in this work, the influences on morphological, optical, and electrical properties of ZnO films by the thickness and deposition temperature of homo-buffer layer during an MBE deposition was explored and discussed on a collective basis, compared with other reports. Characterization tools such as reflection high-energy electron diffraction (RHEED), X-ray diffraction (XRD), field emission scanning electron microscopy (FE-SEM), photoluminescence (PL), and Hall measurement were used for the analysis.

2. Experiments

The ZnO films were deposited by radical source MBE. An elemental Knudsen cell was used to supply zinc atoms of 6 N purity. The temperature of the cell was maintained at 330°C during deposition. Active oxygen species was injected through a radio-frequency (RF) plasma source with the power of 250 W. Before deposition, the *c*-plane sapphire substrates (Kyocera) were cleaned with trichloroethylene, acetone, methanol, and ethanol, and then they were treated in the heated acid solution of H_2SO_4 and H_3PO_4 for 10 min [11].

After the substrate was transferred from the load-lock chamber to the main chamber (base pressure = $1–2 \times 10^{-9}$ Torr), the substrate was thermally cleaned at 800°C for 30 min under an oxygen plasma atmosphere of 1×10^{-4} Torr. The buffer layers were grown at different substrate temperatures ranging from 400°C to 700°C. The thickness of the buffer layer was also varied from 8 to 30 nm. The deposited buffer layers were thermally treated at 800°C for 30 min. Then, the growth was restarted at the same temperature and continued for 4 h. The total thickness of the films was about 100 nm.

RHEED (Oxford Applied Research, LEG 110) patterns were observed to monitor the surface status of the films during deposition. PL and Hall measurements were performed to analyze optical properties and electrical properties, respectively. The crystallinity of the deposited films was estimated by XRD rocking curves (Philips, X-PERT PRO-NMR).

3. Results and discussions

Firstly, the growth mode of the ZnO homo-buffer layer was examined at a different thickness. Fig. 1a shows RHEED patterns from the surfaces of ZnO buffer layer with a different thickness deposited at 500°C. Similar to the observation of GaN/sapphire [12,13] or XRD φ-scan or RBS angular scan of ZnO growth on sapphire [14], a 30° rotation in the basal plane of the ZnO buffer layer was observed by RHEED. The $[1\,\bar{2}\,1\,0]$ direction of ZnO was found to align with $[1\,\bar{1}\,1\,0]$ direction of Al_2O_3 (1 0 0 0).

In the initial stage of the growth, a sharp and streaky pattern was well observed until 10 min growth (which is equivalent of about 5 nm ZnO, not shown here) and this indicates two-dimensional epitaxial growth and is similar to results observed during the growth of GaN on sapphire (0 0 0 1) [15]. As the thickness was increased, the spotty pattern was superimposed on the streaky line, suggesting the growth of the island. In

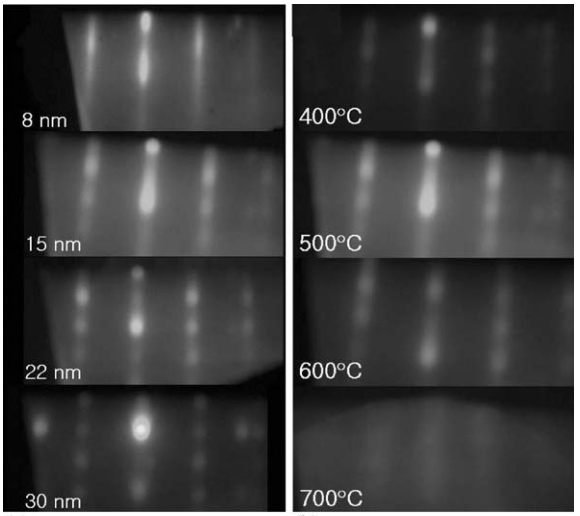

Fig. 1. $\langle 1\bar{2}10 \rangle$ RHEED patterns of the ZnO buffer layers after thermal-treatment for 30 min at 800°C. The thin films were prepared with varying: (a) thickness and (b) deposition temperature.

Fig. 1a, all the RHEED patterns were taken after thermal treatment at 800°C for 30 min with the continuous exposure of oxygen plasma. At the thickness of 8 nm, the diffraction line showed a quite sharp streaky line with very weak spotty pattern, and therefore a two-dimensional growth mode of ZnO buffer layer seemed to be kept up to this thickness. This result agreed with not only the report that a coherently stable layer-by-layer growth of GaN on GaAs by brief plasma exposure was approximately one-monolayer in thickness [16], but also recent report of ZnO grown on sapphire grown by plasma-enhanced MBE [11]. The RHEED pattern from the 15 nm thick buffer layer showed a mixture of thicker line and spotty pattern, indicating the formation of an island. As the thickness was increased, the intensity of the spotty pattern gradually increased, whereas that of the streaky line diminished and almost disappeared at the 30 nm thick ZnO buffer layer. From the results, an initial two-dimensional epitaxial growth continued up to the nominal thickness of 5–8 nm and was quickly followed by three-dimensional nucleation due to large misfit between ZnO and sapphire (~16.7%). The growth mode of the ZnO buffer layer displays an intermediate case, the layer plus 3D island, or Stranski–Krasanov mode.

Secondly, the dependence of the ZnO buffer layer on the growth temperature was studied at the same thickness of 15 nm. As shown in Fig. 1b, RHEED patterns from the ZnO buffer layer grown at temperature 400–600°C have revealed the streaky line superimposed with spotty patterns. As mentioned in Fig. 1a, at this thickness an island growth was already observed. Compared with the ZnO films grown at 400°C, the RHEED line and the intensity of spotty pattern for the film at 500°C were thicker and increased. At an elevated temperature of 600°C, however, the intensity of both the streaky line and spotty patterns were quite weakly decreased. In addition, the diffraction line of the buffer layer deposited at 700°C showed relatively hazy character and the distance between the lines became narrow. The reducing distance between the diffraction patterns denotes that the atomic distance was close to that of Al_2O_3 (0 0 0 1), which has a larger lattice constant than ZnO (0 0 0 1). Consequently, the film thickness of the buffer layer grown at 700°C seemed to be very thin and also the surface of buffer layer became ill ordered. This kind of disordering of the buffer layer might be attributed to a higher desorption rate of impinged atoms on a substrate at a quite elevated deposition temperature.

Fig. 2a presents the surface images of the ZnO films grown at 800°C on different buffer layer thickness. The total film growth time was 3 h 30 min as the overall thickness of the films was fixed around 100 nm. The buffer layer of each condition was deposited at 500°C. The post-growth SEM image of the ZnO on 8 nm buffer layer shows a quite smooth morphology with some scattered crystallites of 35–90 nm size. The surface of the ZnO grown on 15 nm buffer layer became a little rough but still smooth, and the number of the crystallite and their size were reduced. As the buffer thickness increased to 22–30 nm, the surface morphology became aggravated as the size of the crystallite having distorted hexagonal shape became larger and larger.

Fig. 2b illustrates the SEM images of the ZnO films grown at 800°C on the constant buffer layers of 15 nm prepared at the different deposition

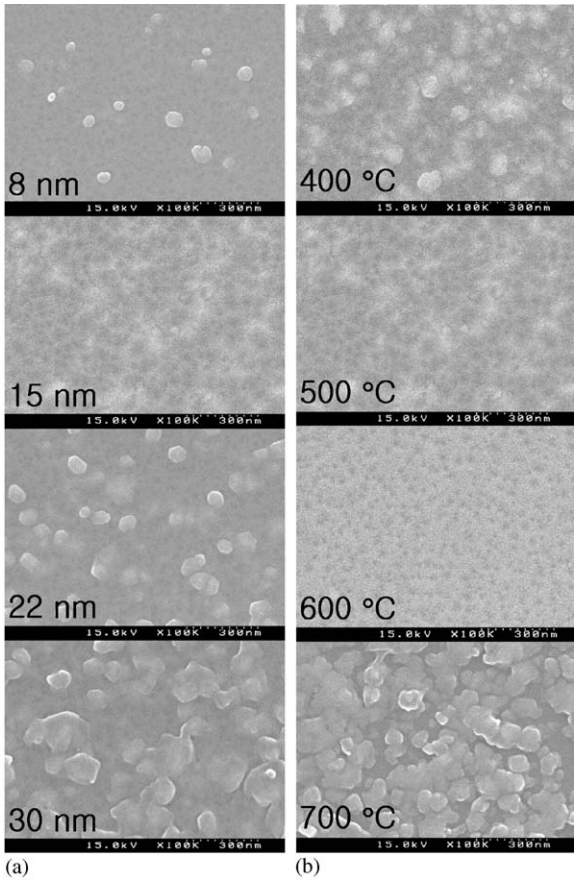

Fig. 2. SEM images of the 100 nm thick ZnO films deposited with (a) the buffer-layer thickness and (b) the different buffer-layer deposition temperature.

temperatures. The buffer layers and upper layers were grown for 30 min and 3 h, respectively. By the SEM images, the surface of the ZnO films grown on the buffer layer deposited at 400°C consisted of many crystallites of ~92 nm in size and was not of smooth morphology. As the temperature for buffer growth increased, the surface became smooth and the size of the crystallite was also diminished. In case of the surface for the ZnO film grown on the buffer deposited at 600°C, no crystallites was found, but instead there existed lots of voids on the surfaces. From the RHEED patterns in Fig. 1b, a mixed streaky and spotty pattern for all the buffer layer of 15 nm deposited at 400–600°C. For the surface microstructure image of the ZnO film grown on the buffer layer prepared at 700°C, lots of crystallites were found and so the surface roughness became irregular. As mentioned before, few ZnO atoms without the formation of 2D layer were deposited for the buffer layer on sapphire surface because of high desorption rate such a high substrate temperature, indicating that the buffer layer might not be well prepared for epitaxial growth. It can be suggested that this kind of atomic-like island buffer led easily to 3D grain growth of the ZnO film growth at the very beginning stage. The rough surface of the ZnO film on the buffer layer grown at 700°C indicates that well-ordered low temperature buffer was very crucial to the growth of the flat surface of upper ZnO films.

Room-temperature PL measurement results are shown in Fig. 3a and b. In Fig. 3b, the intensity of

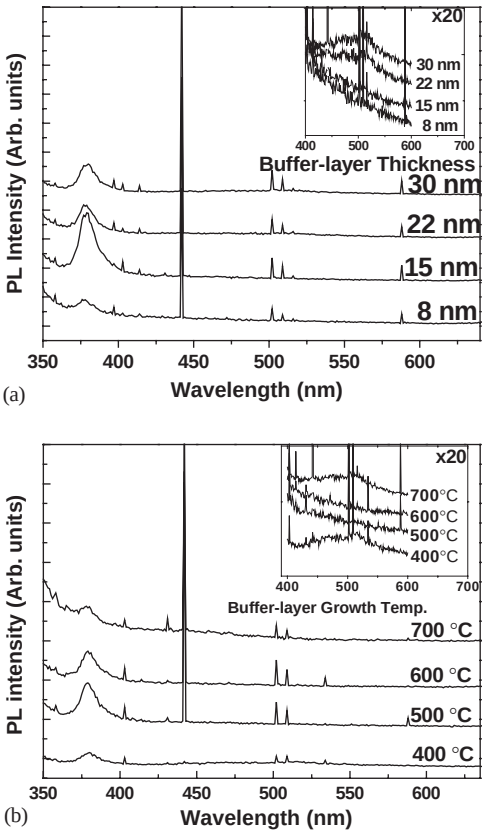

Fig. 3. PL spectra of the ZnO films deposited with: (a) the buffer-layer thickness; and (b) the different buffer-layer deposition temperatures.

near band-edge emission (NBE) at 379 nm (3.278 eV) was increased as the thickness of the buffer layer increased from 8 to 15 nm, and then was slightly decreased and saturated at the thicker buffer layer. From the inset in Fig. 3a, there was no deep-level emission (DLE) for the ZnO films on the buffer layer up to 15 nm, but broad DLE centered around 510 nm (2.436 eV) appeared for the ZnO films on the buffer layers thicker than 22 nm. This result agrees with the observation that the smoothest surface and the weakest deep-level emission in the case of appropriate buffer-layer thickness (about 10 nm) for the ZnO films deposited by a sputtering technique have been reported [10].

Very sharp NBE was found in the ZnO films grown on the buffer layer of 15 nm thick prepared at the temperature of 500–600°C. The graph inserted in Fig. 3b indicates broad DLE for the ZnO films with the buffer deposition temperatures of 400°C and 700°C, whereas any distinctive emission related to a deep level could not be observed over the ZnO films on the buffer layer deposited at intermediate temperatures (500–600°C). It has been reported that deep-level emissions observed at the PL spectra of ZnO films were caused by impurities and native defects [17]. DLE for the ZnO film on the low temperature (400°C) buffer layer happened to result from the underlying buffer layer that might have higher structural defect density because of lower deposition temperatures. From the PL measurement, it can be believed that the weak deep-level emissions observed in the cases of the lower (400°C) or higher (700°C) buffer growth temperature and the thicker buffer-layer films (22 and 30 nm) in the present work might be related to the relatively rough and coarse structures compared with other ZnO films on the buffer layer grown at 500–600°C.

Fig. 4 presents XRD θ-rocking curves of the ZnO (0 0 0 2) diffraction peaks. In Fig. 4a, as the thickness of buffer layer was varied, XRD peak intensities increased with the thickness of buffer-layer thickness. FWHM of the ZnO film on the thickest buffer layer of 30 nm was estimated as the lowest value of 0.6°. The FWHMs values ranged from 0.6° to 0.8° in this research, which were considerably larger than the values reported [9].

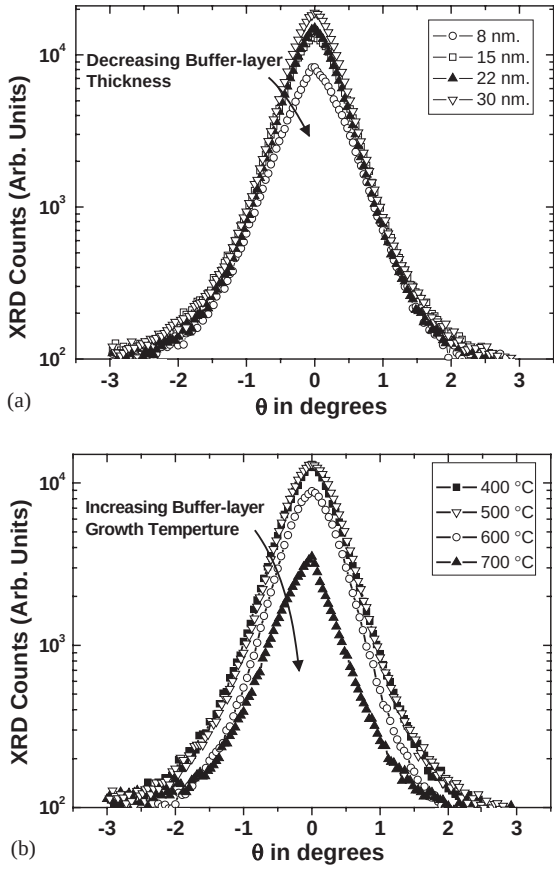

Fig. 4. XRD θ-rocking curves of the ZnO (0 0 0 2) films deposited with: (a) the buffer-layer thickness; and (b) the different buffer-layer deposition temperatures.

This may be because of relatively much lower thickness of the films in this experiment. By increasing the thickness of upper layers up to 1 μm, noticeably smaller FWHM values down to 0.1–0.2° were measured. According to Nakamura et al. the ZnO film grown on the ZnO homo buffer-layer thickness of 50 nm by PLD showed the smallest FWHM value in XRD θ-rocking measurement [9]. The tendency for crystallinity by the ZnO films to be improved with the increment of the buffer thickness might accord with the previous one [9] because their result showed a continuous decrease in FWHM up to the buffer thickness of 50 nm.

When XRD θ-rocking curves were taken over the ZnO films grown on the buffer layer prepared

at a different temperature, the highest peak intensity was observed in the ZnO on the buffer deposited at temperature of 500°C as shown in Fig. 4b. The peak intensity slightly decreased for the ZnO film with the buffer layer deposited at the temperature of 400°C, and significantly decreased at temperature 600–700°C. This result is well consistent with the surface morphology and PL measurement results shown in Figs. 2b and 3b, respectively. Nakamura et al. also reported the optimum buffer growth temperature at 500°C from the lowest full-width at half-maximum (FWHM) values of ZnO films deposited by PLD at the temperature.

Fig. 5a shows the effect of buffer layer thickness on the electrical properties calculated by Hall measurement. The ZnO film with the buffer deposition temperature of 500°C showed the lowest carrier concentration of $6 \times 10^{18}\,cm^3$ while the other ZnO films exhibited high concentration values from 2×10^{19} to $1.2 \times 10^{20}\,cm^3$. This result also indicates that a deep-level emission was closely related to a carrier concentration since the ZnO films with larger thickness than 22 nm showed deep level emissions and higher carrier concentrations likewise. The reason for showing the high mobility as large as $\mu = 40-57\,cm^2/V\,s$ of the ZnO film on thicker buffer layers of 22–30 nm can be attributed to better crystalline quality of these samples analyzed through XRD rocking curves in Fig. 4a.

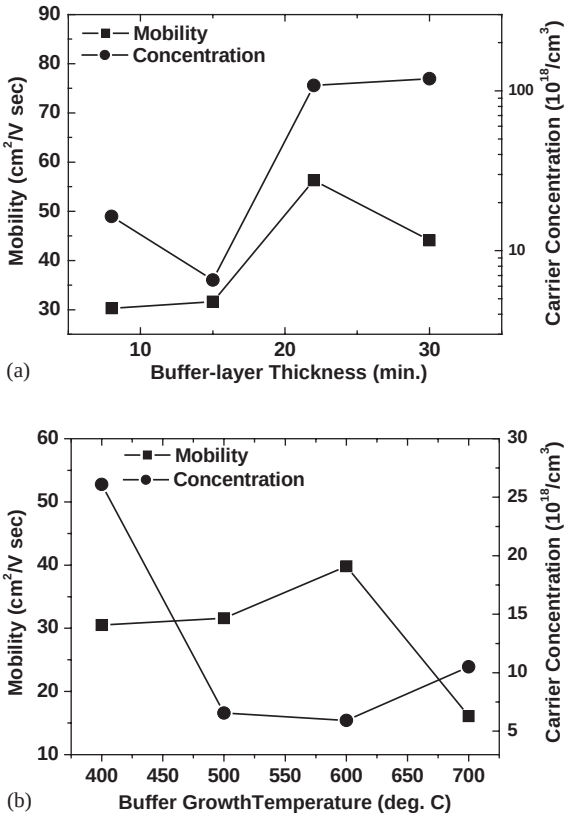

Fig. 5. Hall measurement results of the ZnO films deposited with: (a) the buffer-layer thickness; and (b) the different buffer-layer deposition temperatures.

Fig. 5b presents the effect of buffer growth temperature on the electrical properties calculated by Hall measurement. The data show that the buffer deposition conditions of moderate temperatures (500–600°C) led to higher Hall mobility values and lower carrier concentrations. These results were consistent with the PL measurement data since deep-level emissions were observed for the samples that have a higher carrier concentration (Buffer growth temperature = 400°C or 700°C).

4. Conclusion

The effects of buffer-layer deposition conditions on the properties of the ZnO films deposited by plasma-assisted MBE were explored. When ZnO homo buffer layer was prepared at different temperatures and thicknesses, RHEED patterns for ZnO buffer layer showed very streaky lines until 5–8 nm and then quickly turned into the mixed pattern of both streaky and spotty patterns. This means that growth mode of ZnO thin film on sapphire showed conventional Stranski–Krastanov mode due to a large lattice misfit between ZnO and c-Al_2O_3 (0 0 0 1). This intermediate growth mode was supported by the observation of scattered crystallites on all the ZnO thin film of 100 nm thick deposited on different buffer layers. In PL measurement at room temperature, only strong NBE could be observed on the ZnO films grown on the very smooth surface of the buffer layer prepared at the temperature of 500–600°C with 8–15 nm thickness. The ZnO films grown on

the buffer layer thicker than 15 nm and prepared at a low temperature of 400°C or a high temperature 700°C exhibited DLE centered around 510 nm. From the analysis of the XRD rocking curve of the ZnO (0 0 0 2), the ZnO film grown on the 15 nm buffer layer prepared at 500°C showed the smallest value of FWHM, which was continuously decreased as the buffer thickness increased from 8 to 30 nm. In Hall measurement, the carrier concentration was revealed to correlate with the deep-level emission in PL and the ZnO films grown on the buffer layer with 22–30 nm thick having good crystalline quality showed a high mobility of $\mu = 40-57\,\mathrm{cm}^2/\mathrm{V\,s}$.

Acknowledgements

This work was partially supported by KIST Future-Resource Program Grant No. 2E17733.

References

[1] D.M. Bagnall, Y.F. Chen, Z. Zhu, T. Yao, S. Koyama, M.Y. Shen, T. Goto, Appl. Phys. Lett. 70 (1997) 2230.
[2] X.L. Guo, J.H. Choi, H. Tabata, T. Kawai, Jpn. J. Appl. Phys. 40 (2001) L177.
[3] P. Yu, Z.K. Tang, G.K.L. Wong, M. Kawasaki, A. Ohtomo, H. Koinuma, Y. Segawa, Solid State Commun. 103 (1997) 459.
[4] D.C. Reynold, D.C. Look, B. Jogai, H. Morko, Solid State Commun. 101 (1997) 643.
[5] N. Ohshima, H. Yonezu, S. Yamahira, K. Pak, J. Crystal Growth 189–190 (1998) 275.
[6] W.K. Fong, C.F. Zhu, B.H. Leung, C. Surya, J. Crystal Growth 233 (2001) 431.
[7] S. Nakamura, G. Fasol, The Blue Laser Diode, Springer, Berlin, 1997, p. 63.
[8] K. Nakahara, H. Takasu, P. Fons, K. Iwata, A. Yamada, K. Matsubara, R. Hunger, S. Niki, J. Crystal Growth 227–228 (2001) 923.
[9] T. Nakamura, Y. Yamada, T. Kusumori, H. Minoura, H. Muto, Thin Solid Films 411 (2001) 60.
[10] K.H. Bang, D.K. Hwang, J.M. Myoung, Appl. Surf. Sci. 207 (2003) 359.
[11] Y. Chen, D.M. Bagnall, Z. Zhu, T. Sekiuchi, K.T. Park, K. Hiraga, T. Yao, S. Koyama, M.Y. Shen, T. Goto, J. Crystal Growth 181 (1997) 165.
[12] R.D. Vispute, V. Talyansky, Z. Trajanovic, S. Choopun, R.P. Sharma, T. Venkatessan, Appl. Phys. Lett. 73 (1998) 348.
[13] M. Johnson, S. Fuzita, W. Rowland Jr., W. Hughes, J. Cook Jr., J. Schetzina, J. Electron. Mater. 25 (1996) 855.
[14] K.K. Kim, J.-H. Song, H.-J. Jung, S.J. Park, J.H. Song, J.H. Lee, W.K. Choi, J. Vac. Sci. Technol. A 18 (2000) 2864.
[15] R.C. Powell, N.-E. Lee, Y.-K. Kim, J.E. Greene, J. Appl. Phys. 73 (1993) 189.
[16] R.J. Auenstein, D.A. Collins, X.P. Cai, M.L. O'Steen, Appl. Phys. Lett. 66 (1995) 2861.
[17] D.C. Reynold, D.C. Look, B. Jogai, H. Morko, Solid State Commun. 106 (1998) 701.